Chapter 14
Remote Sensing of Aerosols by Sunphotometer and Lidar Techniques

Anna M. Tafuro, F. De Tomasi, and Maria R. Perrone

Abstract Active and passive remote sensing devices such as lidars and sunphotometers, respectively, are peculiar tools to follow the spatial and temporal evolution of aerosol loads and get complementary data to properly characterize aerosol optical and microphysical properties. A XeF-based Raman lidar is routinely used at the physics department of Lecce's University (40° 20′ N, 18° 6′ E), to monitor aerosol vertical distributions and characterize aerosol optical properties by the vertical profiles of the backscatter and extinction coefficient, lidar ratio, and depolarization ratio. In addition, a sun/sky radiometer operating within AERONET is used to supplement lidar measurements and better infer aerosol types and properties by columnar values of the particle size distribution, the real and imaginary refractive index, the single scattering albedo and the Angstrom exponent (Å). The main objective of this paper is to provide some results on the spatial and temporal evolution of the aerosol properties over south-east Italy, in the central-east Mediterranean basin, by using lidar and sunphotometer measurements. Specifically, results on the characterization of the aerosol load from July 18 to July 21, 2005 are reported and particular attention is devoted to the Sahara dust outbreak that has occurred over south-east Italy on July 18 and 19, 2005.

Keywords: Aerosols, lidar, remote sensing, sunphotometer

14.1 Introduction

Several studies have shown that both natural and anthropogenic aerosols have important effects on the climate of the earth-atmosphere system (Haywood and Shine 1997). Aerosol particles affect the climate directly by scattering and absorbing solar radiation and indirectly by modifying cloud microphysical properties. But, as a consequence of their high spatial and temporal variability, these effects can

CNISM, Dipartimento di Fisica, Università di Lecce, via per Arnesano, Lecce, Italy

Y.J. Kim and U. Platt (eds.), *Advanced Environmental Monitoring*, 179–189.
© Springer 2008

be strongly regional (Nakajima et al. 2003) and the current uncertainty in the quantitative assessment of the Earth's radiative balance, is a direct consequence of the variable nature of aerosols on regional and seasonal scales. A multiple-measurement approach is currently used to assess aerosol impacts on global climate. Specifically, long-term continuous observations from satellites, networks of ground-based instruments and dedicated field experiments in clean and polluted environments are used to feed global aerosol and climate models (Kaufman et al. 2002). The aerosol robotic network (AERONET), which is an international network coordinated by the NASA Goddard Space Flight Center, has been established to assess aerosol optical properties from ground-based sun/sky radiometer measurements (Holben et al. 1998). The need of assessing a vertical resolved aerosol climatology has led to the establishment of the European aerosol research lidar network (EARLINET) that at present consists of a network of 22 lidar stations spread over whole Europe (Bösenberg et al. 2003).

In this paper, an elastic-Raman lidar operating within EARLINET and a sun/sky photometer operating within AERONET are used to characterize the aerosol load from July 18 to July 21, 2005. Particular attention is devoted to the Saharan dust event occurred in the south-east of Italy on July 18–19. A main paper's objective is to show that complementary measurements are required to infer optical and microphysical properties of aerosols of different type. Measurements have been performed at the physics department of Lecce's University that is located on a flat peninsula of south-east Italy, nearly 50 km away from large industrial areas. The site is well suited to contribute to the aerosol characterization of the east Mediterranean basin, which represents a unique area in terms of suspended particulate matter. Aerosols from different sources converge to the Mediterranean basin: urban/industrial aerosols and seasonal biomass burning from Europe (Zerefos et al. 2000; Lelieveld et al. 2002), maritime and long-range transported polluted air masses from the Atlantic Ocean, mineral dust from North Africa (Gobbi et al. 2000; Tafuro et al. 2006), and sea spray from the Mediterranean sea itself (Perrone et al. 2005). A brief description of the XeF lidar and of the sunphotometer is given in Section 14.2. The advection pattern characterization over south-east Italy from July 18 to July 21, 2005 is provided in Section 14.3 by using 7-day analytical backtrajectories and satellite MODIS images. Lidar and sunphotometer measurements are analyzed in Sections 14.4 and 14.5, respectively. Summary and conclusion are reported in Section 14.6.

14.2 Experimental Facilities

An elastic-Raman lidar employing a XeF excimer laser (Lambda Physik LPX 210 I) as radiation source has been used in this study for the aerosol vertical monitoring. The lidar system is located at the physics department of Lecce's University (40° 20′ N, 18° 6′ E), on a flat area of the Salento peninsula in Italy. The XeF laser emits light pulses of 30 ns duration at 351 nm, with a maximum energy and repetition rate of 250 mJ and 100 Hz, respectively. Collection of the backscatter radiation is

obtained by a Newtonian telescope, whose primary mirror has 30 cm-diameter and 120 cm-focal length. The lidar system has been designed to measure as a function of the altitude, the aerosol backscatter coefficient, the extinction coefficient, the extinction-to-backscatter ratio, known as lidar ratio, the depolarization ratio, and the water vapor mixing ratio. More details on the experimental apparatus are reported in De Tomasi and Perrone (2003).

A sun/sky radiometer made by CIMEL (France) and operating within AERONET has been used to derive columnar values of the aerosol size distribution, the real and imaginary parts of the complex refractive index, the single scattering albedo, and the aerosol optical thickness. The CIMEL sunphotometer (CE318-1) is an automatic sun/sky radiometer, with a 1.2° field of view and two detectors, to measure direct Sun and sky radiances at eight spectral channels: 340, 380, 440, 500, 670, 870, 940, and 1020 nm. Holben et al. (1998, 2001) have provided a detailed description of the instrument, the data acquisition system and the data inversion procedure. The instrument is located on the roof of the physics department of Lecce's University.

14.3 Characterization of Advection Patterns by Backtrajectories and Satellite Images

The 7-day analytical backtrajectories and MODIS satellite images have been used to infer the source regions of the air masses advected over south-east Italy from July 18 to July 21, 2005. The 7-days backtrajectories, for seven distinct arrival height levels (950, 850, 700, 500, 300, 250, and 200 hPa) and for two arrival times (00:00 and 12:00 UTC), are provided by NASA for each AERONET site (http://croc.gsfc.nasa.gov/aeronet/index.html). Figure 14.1 shows the 7-day analytical backtrajectories of the air masses reaching the monitoring site on (a) July 18 at 12:00 UTC, (c) July 19 at 00:00 UTC, and (e) July 21 at 00:00 UTC, respectively. Figure 14.1a indicates that on July 18, at 12:00 UTC, the 950 and 850 hPa air masses have been advected to Lecce from Europe, while the 700 hPa air mass has been advected from the Atlantic Ocean. Figure 14.1b shows as function of time, the change of height of the 950, 850, and 700 hPa air masses for the 12:00 UTC arrival time.

Figure 14.1c, which displays the July 19 backtrajectories, indicates that north-west Africa was the source region of the 700 hPa air mass advected to Lecce on July 19, while Fig. 14.1d shows as function of time, the change of height of the 950, 850, and 700 hPa air masses, for the 00:00 UTC arrival time, and we observe that the air mass reaching Lecce on July 19 at about 700 hPa, was at ~900 hPa over north-west Africa. Hence, this air mass is expected to be affected by Sahara dust particles. Last conclusion is supported by satellite images.

Figures 14.2a and 14.2b show two MODIS images of the central Mediterranean provided by the Aqua satellite (http://rapidfire.sci.gsfc.nasa.gov/) for July 18 at 12:00 UTC and for July 19 at 12:40 UTC, respectively. It is worth observing from Fig. 14.2a that a dust plume, moving from Sahara, was present over the south-west Mediterranean on July 18, at midday. Then, according to the backtrajectories of

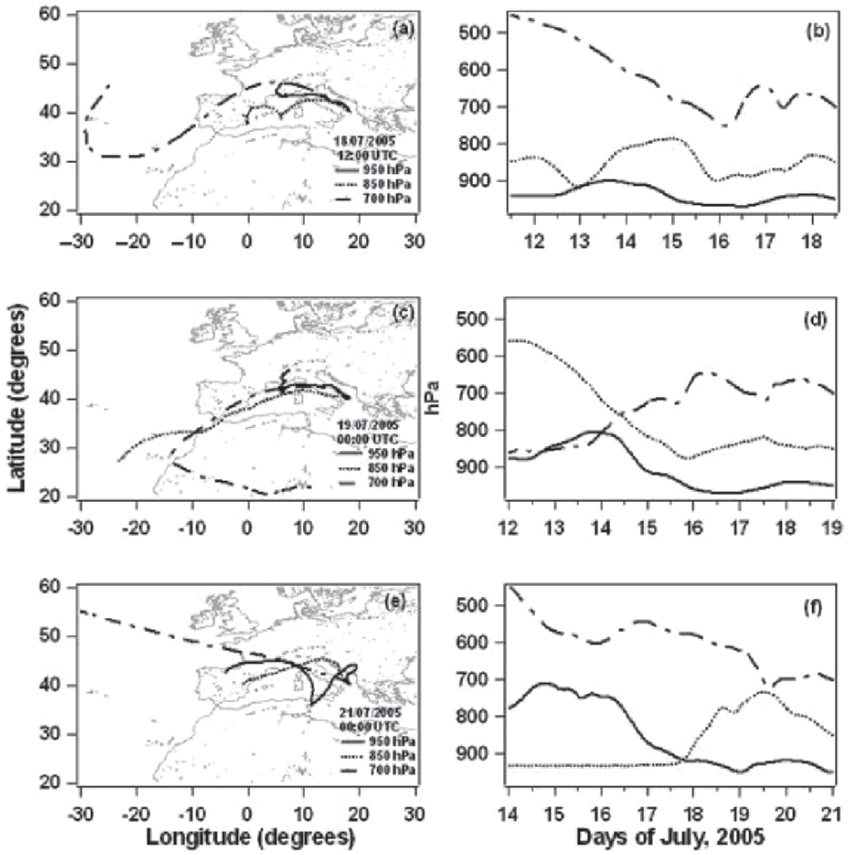

Fig. 14.1 7-days analytical back trajectories for the air masses reaching Lecce on (**a**) July 18 at 12:00 UTC, (**c**) July 19 at 00:00 UTC, and (**e**) July 21 at 00:00 UTC. The change of the height of the 950, 850 and 700 hPa air masses as function of time is also shown for the arrival time of (**b**) 12:00 UTC of July, 18, (**d**) 00:00 UTC of July 19, (f) 00:00 UTC of July 21

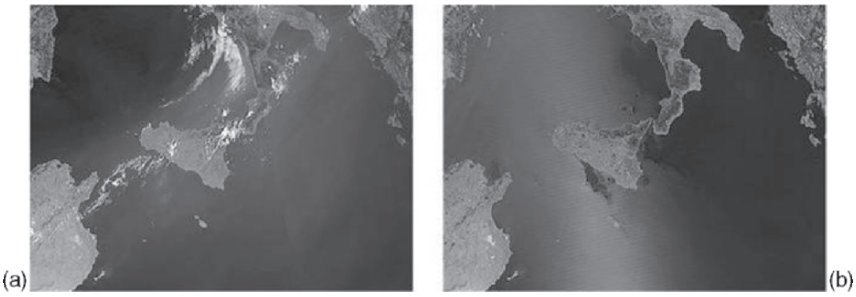

Fig. 14.2 MODIS image of the Mediterranean from Aqua satellite on (**a**) 18 and (**b**) 19 July, 2005 at 12:00 and 12:40 UTC, respectively

Fig. 14.1d, Fig. 14.2b indicates that the dust plume was over south-east Italy on July 19 at 12:40 UTC. Finally, it is also worth noting from Fig. 14.1e that north-west Europe was the source region of the 950 and 850 hPa air masses that have reached Lecce on July 21, while the Atlantic Ocean was the source region of the 700 hPa air mass.

In conclusion, the analysis of backtrajectories and satellite images indicates that aerosols of different type and from different source regions have been advected to Lecce from July 18 to July 21, 2005.

14.4 Aerosol Characterization by Lidar Measurements

Lidar techniques have the unique feature of retrieving vertical resolved aerosol properties. This is particularly useful because passive remote sensing techniques can give only column-averaged aerosol quantities. Aerosol characteristics have been monitored almost continuously on July 18 and July 21. The daily evolution of the backscatter coefficient retrieved from lidar measurements performed from 8:20 to 19:20 UTC of July 18, is shown on Fig. 14.3. The backscatter coefficient is retrieved by the Klett inversion technique (Fernald 1984), that requires a hypothesis on the extinction-to-backscatter coefficient ratio. The lidar ratio depends on size distribution, shape and chemical composition of particles and as a consequence it allows characterizing aerosols of different origin and type (Ackermann 1998; Matthias and Bösenberg 2002). It generally increases with decreasing particle size and increasing contribution to light extinction (Ansmann et al. 2001). Literature values of lidar ratios range from about 10 to 150 sr (Barnaba et al. 2004). According to published works, lidar ratios in the range 50–80 sr can be representative of

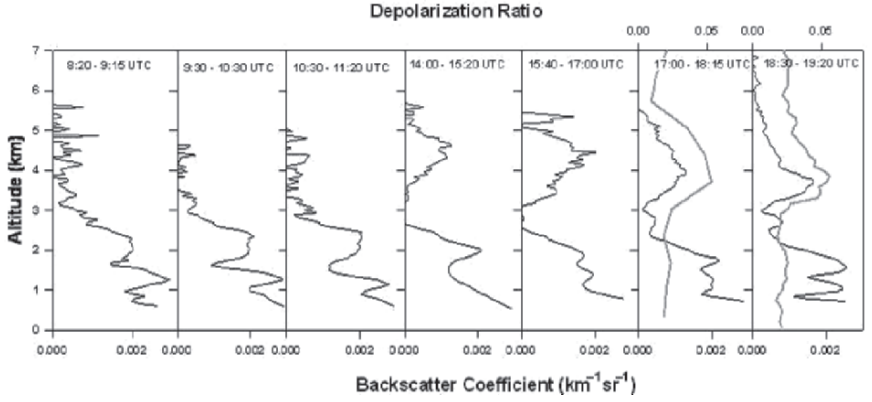

Fig. 14.3 Backscatter coefficient vertical profiles retrieved by lidar measurements on July 18, 2005. Grey lines provide depolarization ratio vertical profiles

non-spherical dust particles and of small absorbing particles (Mishchenko et al. 1997; Mattis et al. 2002; Perrone et al. 2004).

We have set the lidar ratio to 80 sr, to retrieve the backscatter coefficient plotted in Fig. 14.3 This choice will be explained later in. Fig. 14.3 shows that the aerosol vertical distribution varies significantly during July 18. Aerosols are confined at altitudes below 3 km in the morning, while a separate aerosol layer appears from ~14:00 UTC until the evening above 3 km. According to backtrajectories (Fig. 14.1) and satellite images (Fig. 14.2), it is very likely that the higher layer is made of Saharan dust that reaches south-east Italy on the afternoon of July 18. This conclusion is supported by the depolarization ratio measurements (Fig. 14.3, grey lines). The depolarization ratio is the ratio between the total cross-polarized backscatter coefficient and the total polarization preserving backscatter coefficient; it has a value of 0.014 in a pure molecular atmosphere and generally higher values in presence of aerosols. Specifically, spherical particles produce low depolarization ratios, while depolarization ratios larger than 10–15% are associated to non spherical particles such as desert dust particles (Tafuro et al. 2006). We observe from Fig. 14.3 (grey lines) that the aerosol layer above 3 km of altitude is characterized by a depolarization ratio larger than that of the lower altitude aerosol layer. Hence, latter results may indicate either a large presence of non-spherical dust particles on the upper aerosol layer and that the lowermost aerosol layer is mostly made of spherical particles. Our lidar system allows depolarization ratio measurements only on late afternoons, when the solar background is not too high compared to the weak depolarized signal.

Figure 14.4a shows the vertical profiles of the backscatter and extinction coefficient, and of the lidar ratio that have been retrieved by Raman lidar measurements performed on July 18 from 20:50 to 22:15 UTC. The backscatter and extinction coefficient vertical profiles of Fig. 14.4a also reveal the presence of two aerosol layers: one between 2.5 and 5.5 km and the other below 2 km of altitude. However, it is worth noting from Fig. 14.4a that the lidar ratio takes value of ~80 sr from about 1 to 5 km: the upper and lower aerosol layers are characterized by rather close lidar ratio values, even if in accordance to depolarization ratios, the two aerosol layers are expected to be made of particles of different microphysical properties. As we have mentioned, large non-spherical dust particles and small absorbing particles can both be characterized by high lidar ratios.

The nighttime Raman lidar measurements of July 18 have been taken into account to set the lidar ratio to 80 sr and retrieve diurnal backscatter coefficient profiles (Fig. 14.3). In particular, we have assumed that the aerosol layer monitored by the lidar during the day hours is characterized by a lidar ratio value equal to that of the lowermost aerosol layer of Fig. 14.4a. According to depolarization ratio vertical profiles (Fig. 14.3, grey lines), the lowermost layer appears to have not been affected by the dust plume located above ~2 km of altitude.

Lidar measurements have also been performed on July 21, but are not available for July19 and 20. Figure 14.5 shows the backscatter coefficient profiles retrieved on July 21 at different day hours. Grey lines on Fig. 14.5 represent depolarization ratio vertical profiles. Nighttime Raman lidar measurements performed on July, 21

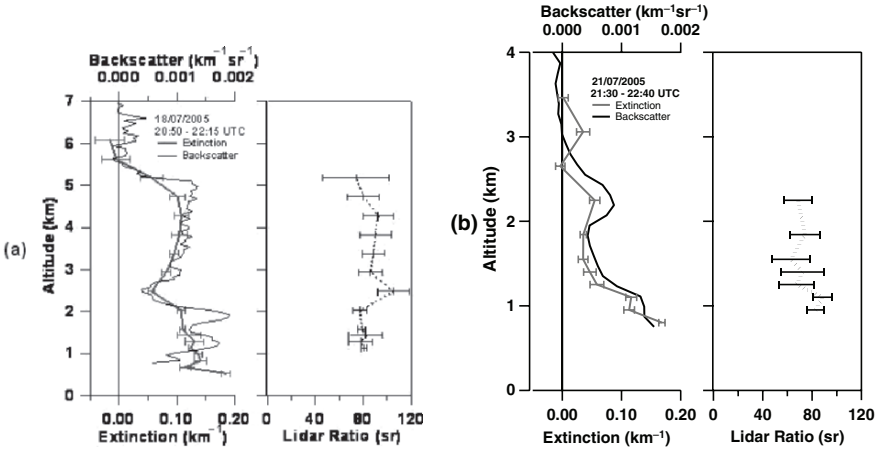

Fig. 14.4 Vertical profiles of the backscatter and extinction coefficient, and of the lidar ratio retrieved by Raman lidar measurements (**a**) on July 18 and (**b**) on July 21 at night

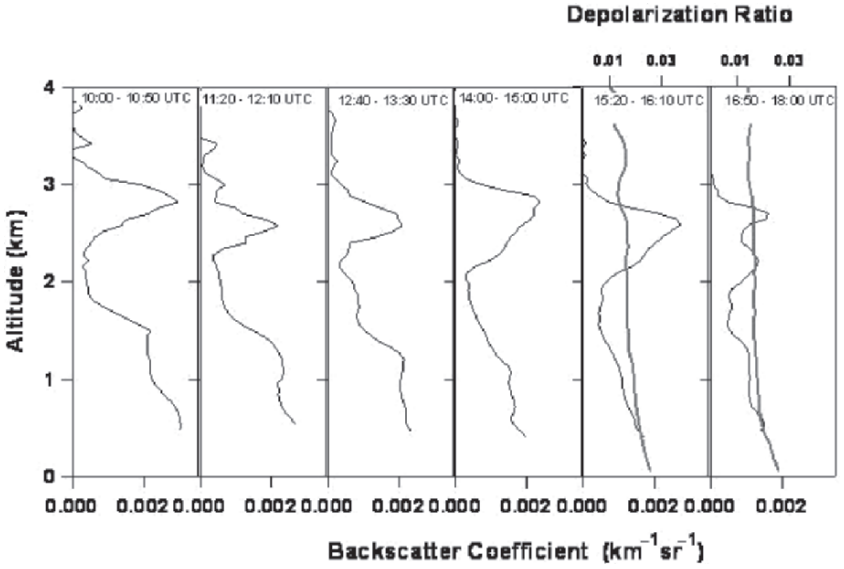

Fig. 14.5 Backscatter coefficient vertical profiles retrieved by lidar measurements on July 21, 2005. Grey lines provide depolarization ratio vertical profiles

from 21:30 to 22:40 UTC are shown on Fig. 14.4b. The lidar profiles of Figs 14.5 and 14.4b reveal the presence at least of two aerosol layers during all measurement hours: one between 2 and 3 km and the other below 2 km of altitude. It is worth noting from Fig. 14.5 that depolarization ratios take, above 2 km of altitude, values that are significantly smaller than those of Fig. 14.3. Latter results may indicate that

the layer monitored on July 21 between 2 and 3 km is likely not due to the presence of non-spherical dust particles, in accordance to backtrajectories (Fig. 14.1) even if the lidar ratio values are about 70 sr from ~1 to 2.5 km of altitude (Fig. 14.4b).

14.5 Aerosol Characterization by Sunphotometer Measurements

AERONET sunphotometer retrievals provide column-averaged aerosol quantities that are rather useful to define aerosol microphysical and optical properties. Figure 14.6 shows the daily evolution of the aerosol optical thickness (AOT) at 440 nm (black symbols) and of the Angstrom coefficient (Å), computed from AOT values at 440 and 870 nm (grey symbol) from July 18 to July 21. Both aerosol parameters vary significantly from July 18 to July 21. The AOT increases from ~0.25 to 0.4 on the afternoon of July 18, takes values between 0.4 and 0.5 on July 19, and decreases up to ~0.3 on the following day. In addition, Å takes values within the 1.7–1.8 range up to ~11:00 UTC and values spanning the 0.8–0.9 range from 15:00 to 18:00 UTC (Fig. 14.6, grey symbols). The Angstrom coefficient temporal evolution allows inferring that aerosols of different type have been advected over the monitoring site on the afternoon of July 18. Å is the best marker to infer changes of columnar microphysical aerosol properties (Tafuro et al. 2006): typical values range from 1.5 for particles dominated by accumulation mode aerosols, to nearly zero for large dust particles. Thus, the Å daily evolution further more indicates that large size particles as those coming from the Sahara desert have been advected over the central-east Mediterranean basin in the afternoon of July 18, in accordance to lidar measurements (Fig. 14.3). This interpretation is also supported by the evolution of the AOT_{fine} to AOT_{coarse} ratio plotted on Fig. 14.7, where AOT_{fine} and AOT_{coarse} represent the aerosol optical thickness due to particles with radius

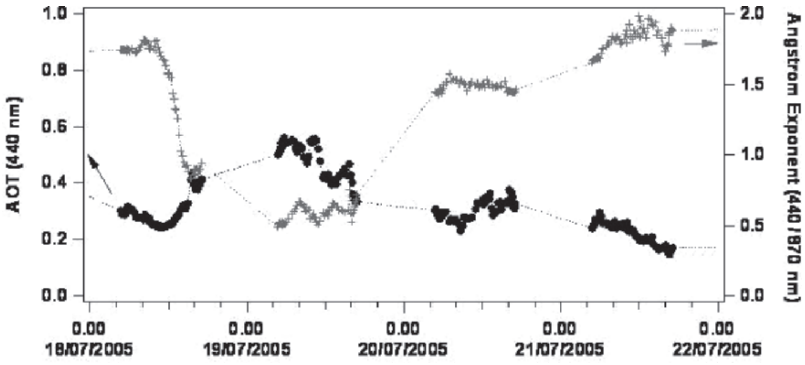

Fig. 14.6 Daily evolution of the optical thickness at 440 nm and of the Angstrom coefficient (440/870 nm).

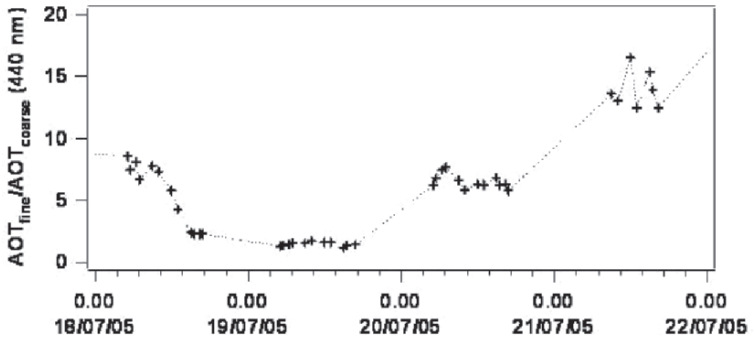

Fig. 14.7 Daily evolution of the AOT_{fine} to AOT_{coarse} ratio

smaller and larger than 0.6 μm, respectively. We observe from Fig. 14.7 that the contribution of fine mode particles that decreases on July 18, increases on July 20 and gets quite large on July 21, as a consequence of the change of the columnar aerosol properties. Hence, sunphotometer retrievals also indicate the advection over south-east Italy of Sahara dust particles from the afternoon of July 18. In addition, they reveal that the Sahara dust outbreak interested Lecce for about 24 h: Å, AOT, and AOT_{fine}/AOT_{coarse} again take values close to those before the dust outbreak on July 20.

A significant increase of the AOT during the dust outbreak is also revealed by Fig. 14.6 (black symbols). It is worth mentioning that the aerosol optical thickness at 351 nm, calculated from the aerosol extinction profile, retrieved by the lidar measurements performed on July 18, from 20:50 to 22:15 UTC, which is equal to 0.58 ± 0.02, is in satisfactory accordance with the AOTs retrieved by the sunphotometer measurements on July 18 at 16:20 UTC, and on July 19 at 05:30 UTC, which are 0.50 ± 0.01 and 0.61 ± 0.01, respectively at 440 nm.

It is now interesting to compare lidar and sunphotometer measurements retrieved after the dust event of July 18–19. Figure 14.6 (grey symbols) reveals that, on July 21, the columnar Angstrom coefficient has recovered to the values 1.5–2 observed before the dust event. According to Fig. 14.7, latter result indicates that the size distribution is again dominated by fine mode particles. However, lidar measurements again show the presence of a separate aerosol layer between 2 and 3 km (Figs 14.5 and 14.4b) whose vertical distribution varies during the day. The depolarization ratio is very small in this layer (Fig. 14.5, grey line) and as we have mentioned, this result suggests that the aerosol layer is likely not due to the presence of non-spherical dust particles. Figure 14.1e indicates that air masses from the Atlantic Ocean arrive to Lecce at about 3 km of altitude (700 hPa) on July 21. However, the particle layer revealed by the lidar at 2–3 km can have been lofted inside Europe, in accordance with Fig. 14.1f. Then, this aerosol layer could be due to the presence of small absorbing particles coming from west European industrial areas or from North

America. Lidar ratio values of Fig. 14.7 support the hypothesis that the aerosol layer is made of small absorbing particles (e.g. De Tomasi and Perrone 2003).

We can see from this example that care must be taken when trying to attribute an origin to aerosol layers in the free troposphere: in this case, if only lidar measurements would have been available, the layer at 2–3 km observed by the lidar on July 21, could easily be confused with a residual layer due to the Saharan outbreak occurred two days before. But, the use of different sources of experimental and modeling information has allowed us to better define the origin and the microphysical proprieties of the investigated aerosol layer.

14.6 Summary and Conclusion

A lidar and a sun/sky radiometer have been used to follow the spatial and temporal evolution of the aerosol load over south-east Italy and get complementary data to properly characterize optical and microphysical properties and the vertical distribution of the aerosol particles. It is rather important to characterize, besides aerosol vertical distributions, microphysical properties of the main aerosol layers, because the aerosol radiative forcing is quite dependent on location and properties of the different aerosol layers. Paper's results have shown that the dust transport from Sahara is, in many cases, characterized by a defined layer above the boundary layer. In addition, it has been shown that particularly during Sahara dust outbreaks, the aerosol vertical distribution can change significantly within few hours and as consequence the aerosol radiative forcing may also vary significantly within few hours.

Specifically, the temporal and spatial evolution of the optical and microphysical aerosol proprieties have been investigated from July 18 to July 21, 2005 and particular attention has been devoted to the Sahara outbreak that has occurred over the central-east Mediterranean from July 18 to July 19. It has been shown that the Angstrom coefficient and the AOT_{fine}/AOT_{coarse} ratio represent the best parameters to trace changes of the aerosol columnar content: their respective values have significantly decreased during the advection of Sahara dust particles. Lidar depolarization ratio measurements have allowed inferring the vertical distribution of non-spherical dust particles that are also responsible of the high lidar ratio values that characterize dust layers (Mishchenko et al. 1997). It has also been shown that fine mode particles can lead to high lidar ratios, but in the latter case depolarization ratios much smaller than those observed during dust outbreaks have been found. The significant support of bactrajectories and satellite images to infer the source region of the monitored aerosols has also been demonstrated.

Acknowledgements This work has been supported by Ministero dell'Istruzione dell'Università e della Ricerca of Italy (Programma di Ricerca 2004. Prot. 20004023854) and by the European Project EARLINET-ASOS (2006–2010, contract n. 025991). Results presented in this paper have been obtained using data from the Aerosol Robotic Network (AERONET). The authors kindly thank the AERONET team.

References

Ackermann J. (1998), The extinction-to-backscatter ratio of tropospheric aerosol: A numerical study, *J. Atmos. Ocean. Technol*., 15, 1044–1050.

Ansmann A., Wagner F., Althausen D., Muller D., Herber A., and Wandinger U. (2001), European pollution outbreaks during ACE 2, Part I: Alofted aerosol plumes observed with Raman lidar at the Portuguese coast, *J. Geophys. Res.,* 106 D, 20723–20733.

Barnaba F., De Tomasi F., Gobbi G.P., Perrone M.R., and Tafuro A. (2004), Extinction versus backscatter relationships for lidar applications at 351 nm: Maritime and desert aerosol simulations and comparison with observations, *Atmos. Res*., 70, 229–259.

Bösenberg J., et al. (2003), A European aerosol research lidar network to establish an aerosol climatology, MPI-Report 348*,* Max-Planck-Institut für Meteorologie, Hamburg, Germany.

De Tomasi F. and Perrone M.R. (2003), Lidar measurements of tropospheric water vapor and aerosol profiles over south-eastern Italy, *J. Geophys. Res*., 108, 4286–4297.

Fernald F.G. (1984), Analysis of atmospheric lidar observations: Some comments, *Appl. Opt.,* 23, 652–653.

Gobbi G.P., Barnaba F., Giorgi R., and Santacasa A. (2000), Altitude-resolved properties of a Saharan-dust event over the Mediterranean, *Atmos. Environ*., 34, 5119–5127.

Haywood J.M. and Shine K.P. (1997), Multi-spectral calculations of the direct radiative forcing of the tropospheric sulphate and soot aerosols using a column model, *Q. J. R. Meteorol. Soc.,* 123, 1907–1930.

Holben B.N., et al. (1998), AERONET – A federate instrument network and data archive for aerosol characterization, *Remote Sens. Environ.,* 66, 1–16.

Holben B.N., et al. (2001), An emerging ground-based aerosol climatology: Aerosol optical depth from AERONET, *J. Geophys. Res.,* 106, 12067–12097.

Kaufman Y.J., Tanré D., and Boucher O. (2002), A satellite view of aerosols in the climate system, *Nature.,* 419, 215–223.

Lelieveld J., et al. (2002), Global air pollution crossroads over the Mediterranean, *Science*, 298, 794–799.

Matthias V. and Bösenberg J. (2002), Aerosol climatology for the planetary boundary layer derived from regular lidar measurements, *Atmos. Res*., 63, 221–245.

Mattis I., Ansmann A., Müller D., Wandinger U., and Althausen D. (2002), Dual-wavelength Raman lidar observations of the extinction-to-backscatter ratio of Saharan dust, *Geophys. Res. Lett*., 29, No. 9, 20.1–20.4.

Mishchenko M.I., Travis L.D., Kahn R.A., and West R.A. (1997), Modeling phase functions for dust-like tropospheric aerosols using a shape mixture of randomly oriented polydisperse spheroids, *J. Geophys. Res*., 102, 16, 831–16,847.

Nakajima T., Sekiguchi M., Takemura T., Uno I., Higurashi A., Kim D., Sohn B-.J., Oh S. N., Nakajima T.Y., Ohta S., Okada I., Takamura T., and Kawamoto K. (2003), Significance of direct and indirect radiative forcings of aerosols in the East China Sea region, *J. Geophys. Res*., 108, 8658, DOI 10.1029/2002JD003261.

Perrone M.R., Barnaba F., De Tomasi F., Gobbi G.P., and Tafuro A.M. (2004), Imaginary refractive-index effects on desert-aerosol extinction versus backscatter relationships at 351 nm: Numerical computations and comparison with Raman lidar measurements, *Appl. Opt*., 29, 5531–5541.

Perrone M.R., Santese M., Tafuro A.M., Holben B., and Smirnov A. (2005), Aerosol load characterization over South-East Italy by one year of AERONET sun-photometer measurements, *Atmos. Res.,* 75, 111–133.

Tafuro A.M., Barnaba F., De Tomasi F., Perrone M.R., and Gobbi G.P. (2006), Saharan dust particle properties over the central Mediterranean, *Atmos. Res*., 81, 67–93.

Zerefos C.S., Ganev K., Kourtidis K., Tzortziou M., Vasaras A., and Syrakov E. (2000), On the origin of SO_2 above northern Greece, *Geophys. Res. Lett*., 27, 365–368.